Dissociative Excitation of Some Oxygen-Containing Molecules: Lifetimes and Electron-Impact Cross Sections*

George M. Lawrence

Douglas Advanced Research Laboratories, McDonnell Douglas Corporation, Huntington Beach, California 92647

(Received 25 February 1970)

Decay lifetimes of seven vacuum-ultraviolet O I and O II emission multiplets have been measured using a pulsed electron beam in low-pressure samples of O_2, CO, NO, and H_2O. The lifetimes and cascade patterns of the lines are consistent with known autoionization processes. In two cases, spin-orbit-induced autoionization rates are determined. Absolute electron excitation functions for 8447-Å O I have been measured in the above gases. Relative excitation functions for 1304-Å O I are normalized to the 8447-Å absolute cross section by means of a time-domain cascade analysis. A method for computing relative cross sections from N-exponential decays is outlined.

I. INTRODUCTION

We describe here some measurements of excitation cross sections and decay lifetimes of atomic oxygen emission excited by electron impact on the molecules CO, O_2, NO, and H_2O. The observations reported refer to multiplets with fine structure unresolved. Average wavelengths[1] are used to identify the multiplets.

Dissociative Excitation

The production of excited atomic states by electron impact on molecules can be thought of as excitation to several repulsive potential energy curves of the molecule. In terms of molecular orbitals, one would say that the impact (taking about 10^{-17} sec) excites a transition of a bonding orbital to a nonbonding or weakly bonding orbital. The molecule then dissociates in about 10^{-14} sec into one or more excited atoms. Some such atomic states which radiate by dipole transitions are detected in this experiment.

Excited states of the configuration "$2s\,2p^4$" in O^+ are also produced, presumably by the *ionization* of a $2s\ \sigma$ bonding electron (from O_2).

Useful theory and discussion of dissociative excitation is found in papers on $H(2p)$ production from H_2 by Vroom and DeHeer[2] and by Dunn *et al.*[3] and, for other hydrogen containing molecules, by McGowan *et al.*[4]

Some of the dissociating excited states in O_2 that lead to the atomic emission are seen as background continua in electron energy loss spectra[5,6] and as photodissociation continua.[7] Beyer and Welge[8] have produced 1304-Å O I fluorescence with circa 800-Å radiation onto O_2 and NO.

Sroka[9] has published some excitation functions and spectra for the process $e + O_2$ giving vacuum-uv radiation.

Lifetimes

A recent review of methods for atomic lifetime determinations is given by Ziock.[10] A bibliography[11] and critical data compilations (NBS) of radiative transition probabilities have been made by Wiese and co-workers[12,13] at the National Bureau of Standards. The NBS values for the vacuum-uv transition probabilities treated here have uncertainties of 50% or greater because central-field calculations had to be relied upon at the time of the compilation. Using pulsed electrons in the dissociative excitation process, five O I and two O II decay lifetimes have been measured here with error limits from 3 to 25%.

By a decay lifetime we mean the value τ in an exponential decay, $e^{-t/\tau}$. In two cases (878 Å and 1218 Å), a comparison of the measured τ with the NBS radiative lifetime yields an estimate of the "forbidden" autoionization probability.

The literature values for the 1304-Å O I lifetime show an order-of-magnitude spread and consequently a great amount of effort is spent on this one multiplet.

Absolute Cross Section

In the second part of this paper, we describe the measurement of absolute excitation cross sections for the 8447-Å line of O I using a blackbody as radiation intensity standard. The cross sections for the 1304-Å O I multiplet are then normalized to the 8447-Å cross sections by means of a *cascade analysis* of the 1304-Å time decay curve. Time resolved measurements of excitation functions are discussed by Heddle and Keesing.[14]

II. METHOD: LIFETIMES

Photon decay curves, excited by pulsed electrons, are accumulated in a 256-channel memory of a pulse-height analyzer with the aid of a time-to-

height converter and 100-MHz logic. The apparatus is described in previous papers.[15,16]

The time width of each and every channel of the multichannel analyzer is measured automatically with the aid of a random-pulse source, a crystal time base, and a totalizing scaler. This calibration checks to better than 1% on each channel against a 1% delay line standard and also against a 200.00-MHz sine wave superimposed on the calibration signal. The *average* channel width as determined by the peak in a numerical Fourier transform of the 200.00-MHz sine wave is accurate to 0.05%. In the work reported here, two different source arrangements have been used: a diode with a negative pulse on the cathode and a triode with a positive pulse on the control grid. The triode was constructed to provide a more narrow electron energy distribution than possible with the diode. In operation, a sample gas is introduced, count rate versus wavelength is recorded with dc excitation, a line is isolated with a 1-m monochromator, the electrons are pulsed and a record of the rise and fall of the photon flux is accumulated in the memory of the analyzer. On the resulting digital record (see Fig. 1) four characteristic times must be located by hand before a computer analysis can proceed. In order of increasing time delay, these are the beginning of the time interval, B_1; a point before excitation starts, B_2; a point after excitation is off, t_0; and a point far out in the tail of the decay, t_{FINISH}. The first two parameters (B_1, B_2) define a region of background which is assumed constant over the whole record and is subtracted. The quantities t_0 and t_{FINISH} are the endpoints of an iterative least-squares fit to a sum of two exponentials made by a computer program FRANTIC.[17] The interval from B_2 to t_{FINISH} contains essentially all of the photon "pulse" and is used in the cascade analysis described in the next section. Generally, t_0 is chosen about 1 nsec after the peak of the observed curve. It has been found that the calculated lifetimes and cascade ratios are not sensitive to the exact choice of B_1, B_2, t_0, and t_{FINISH}, for lifetimes greater than 1.2 nsec.

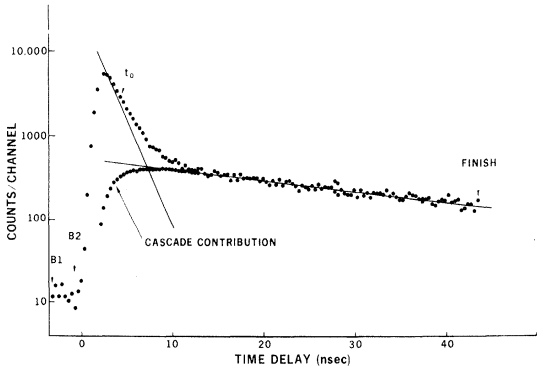

FIG. 1. Sample decay curve for O I 1304 Å. Pulse width was 2 nsec. Electron energy 100 eV. The two straight lines are exponentials determined by FRANTIC. The set of points going up over the peak is the observed decay curve. The points labeled cascade contribution are computed.

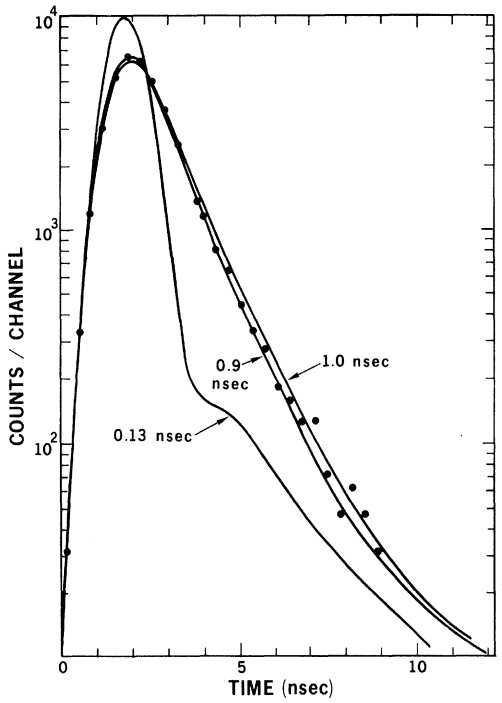

FIG. 2. Decay curves for determining the lifetime of O I 878 Å. Points are observations on 878 Å. The 0.13-nsec curve is the observed Ne II 461 Å pulse. The 0.9- and 1.0-nsec curves are numerical convolutions of 0.9- and 1.0-nsec exponentials with the 0.13-nsec curve.

The lifetimes of the 878-, 1218-, and 718-Å multiplets were too short compared to the system resolution to use the least-squares technique of FRANTIC. For these lines, the system time resolution was determined by recording a decay curve for Ne II, 461 Å. This line has a lifetime of 0.13 nsec as calculated in "multielectron theory" by Westhaus and Sinanoğlu.[18] This Ne II 461-Å decay curve was taken as a measure of the system response and short lifetimes were determined by comparing observed decay curves with the Ne II 461 curve numerically convoluted with various exponentials. The convolution involves integrals similar to that of Eq. (9). Figure 2 indicates the functions involved in finding the 0.9-nsec lifetime for 878 Å. It can be seen in Fig. 2, assuming Ne II 461 Å is cascade free, that the pulsed electron beam has some residual, "longer time scale," decay at about a 1%

TABLE I. Lifetime results.

λ(Å)[a]	Mult.[a]	Classification[a]	τ(nsec) this work	τ(nsec) NBS	τ(nsec) Others
1152 O I	6	$2p^4\ ^1D - 2p^3(^2D^0)3s'\ ^1D^0$	1.9 ±0.2	2.25	
989 O I	5	$2p^4\ ^3P - 2p^3(^2D^0)3s'\ ^3D^0$	4.5 ±0.2	4.35	
878 O I	···	$2p^4\ ^3P - 2p^3(^2P^0)3s''\ ^3P^0$	0.9 ±0.2[b]	3.12	
1218[c] O I	9	$2p^4\ ^1S - 2p^3(^2P^0)3s''\ ^1P^0$	0.9 ±0.2[b]	1.69	
718[c] O II	4	$2s^22p^3\ ^2D^0 - 2s2p^4\ ^2D$	0.4 ±0.1	0.29	0.46[d]
834 O II	1	$2s^22p^3\ ^4S^0 - 2s2p^4\ ^4P$	1.2 ±0.2	0.71	1.45,[d] 1.71[e] ±0.05
1304 O I	2	$2p^4\ ^3P - 2p^3(^4S^0)3s^3S$	1.82 ±0.05	2.63	See text

[a]Reference 1.
[b]Includes effect of forbidden autoionization. Average value for multiplet.
[c]The upper terms have one other downward transition.
[d]Multielectron theory, Ref. 18.
[e]Beam foil, Ref. 33.

level. This causes negligible error.

The system time resolution is limited by electron transit times in the source and in the photomultiplier. It is interesting to note that ~10-psec fluorescence times have been measured[19] using a photon-operated Kerr cell.

III. LIFETIME RESULTS

The seven experimental decay lifetimes are reported in Table I, column 4. They are part of a series of measurements[16,20-24] of vacuum-uv radiative lifetimes. Besides their practical value in aeronomy, plasma studies, and astrophysics, the oxygen lifetimes reported here show some interesting effects associated with autoionization. All the lines but 1304 Å exhibit less than 5% cascading because possible cascading levels are destroyed by autoionization. Absence of cascading has been universally observed[22] in transitions of the type $s^2p^n - sp^{n+1}$. The lines at 1152, 989, 878, and 1218 Å are cases, unique to O I, where levels cascading into 3s states are destroyed by autoionization. The ($3s''$) upper states of the 1218- and 718-Å lines are subject to "forbidden" autoionization which makes the observed decay lifetime shorter than the radiative lifetime. Reference to an O I (and O II) energy-level diagram[25] will be very helpful in understanding the discussions that follow.

878- and 1218-Å O I

The upper terms here are $2p^3(^2P^0)3s''(^3P^0$ and $^1P^0)$, respectively. Since these terms are higher in energy than the $^4S^0$ ionization limit we have to assume that the lifetime will be shortened by autoionization. Since there are no $^1P^0$ or $^3P^0$ terms in the $^4S^0$ continuum, the autoionization will be much weaker than usual.

The 0.9-nsec lifetimes must be considered averaged over all members of the unresolved multiplets.

Encouraged by the fair agreement between the NBS radiative lifetimes and the experimental 1152- and 989-Å lifetimes, we can get the $3s''$ ($^1P^0$ and $^3P^0$) autoionization rates by subtracting the NBS radiative transition probability from the reciprocal of the observed lifetimes. This gives $R_{auto} = (7.9 \pm 2.7) \times 10^8$/sec for the $^3P^0$ term and $R_{auto} = (5.0 \pm 2.8) \times 10^8$/sec for the $^1P_1^0$ level, allowing about 20% error in the NBS radiative transition probabilities. Thus the autoionization rate is roughly the same as the radiation rate and these multiplets exhibit the following properties: (i) the lines are observed in emission; (ii) Huffman *et al.*[26] have observed this multiplet as a set of sharp photoabsorption lines; (iii) Rudd and Smith[27] observed the energy spectrum of autoionizing electrons emitted in heavy particle impact on O_2. Their spectrum contains peaks at the proper energy for $3s''(^3P^0$ and $^1P^0)$ autoionization but the peaks are not resolved from the *LS*-coupling-allowed peaks which are also present; and (iv) Comes *et al.*[28] have observed a sharp peak at 878 Å in the photoionization cross section of atomic oxygen. At this peak, Comes's light source was the 878-Å multiplet of O I which gave resonance absorption with reradiation competing with autoionization.

Some of the theoretical aspects of weak autoionization processes are discussed by Feldman and Novick[29] and *LS*-coupling selection rules are given by Rudd and Smith.[27] In order to get a qualitative understanding of the source of this autoionization for these O I multiplets, a simple calculation of the effect of spin-orbit interaction was performed. The magnetic interaction matrix for the p^3 3s configuration given by Obi and Yanagawa[30] was numerically diagonalized after inserting the parameters determined by Garstang.[31] The dominant effect is due to the spin-orbit parameter ζ which causes the mixing of the $3s''$ ($^1P_1^0$, $^3P_1^0$, and $^3P_2^0$) levels with *S* and *D* terms which do exhibit allowed autoionization. The result of the mixing can be expressed by saying that $\sum_i |\langle {}^1P_1^0,\ {}^3P_1^0 \text{ or } {}^3P_2^0 |$ allowed state

$i\rangle|^2 \sim 10^{-4}$, where the states on the left are the eigenvectors obtained in the matrix diagonalization. If we guess that the allowed autoionization proceeds at a rate of 10^{13}/sec, we would have a rate of 10^9/sec for the spin-orbit-induced autoionization. Thus we can explain the order of magnitude of the observed lifetimes.

A remaining sore point is that the $3s''\ ^3P_0^0$ level has no mixing due to the magnetic interactions. The shape of the decay curve for 878 Å (see Fig. 2), however, limits the presence of any decay with ~ 3-nsec lifetime to less than 5% of the total. It is thus not known to what extent the $^3P_0^0$ level influences the decay curve. Presumably, since the $^3P_0^0$ contains only $\frac{1}{9}$ of the statistical weight of the total $^3P^0$ term, the effect will be small.

1152 and 989 Å

The upper terms here are $2p^3(^2D^0)\,3s'$ ($^1D^0$ and $^3D^0$), respectively. These terms are energetically not subject to autoionization. The observed decay curves exhibit less than 5% cascading which is interpreted as evidence that the cascading levels (np' series) are "destroyed" by autoionization. Although some of the $np' - 3s'$ transitions have been observed in discharges, it would still be expected that the np' levels, being above the $^4S^0$ ionization limit, would be weakened and have their lifetimes shortened by autoionization.

Fair agreement is obtained with the NBS lifetimes which are derived from central-field calculations. This is to be contrasted with the case of the C I "resonance" lines where extensive configuration mixing[32] is required to remove a factor-of-2 discrepancy between central-field theory and experiment.

718- and 834-Å O II

These multiplets in the O II spectrum come from excited states of O^+ classified as from the configuration $2s2p^4$. Such states have without exception been observed to be cascade free in the sense of not exhibiting long-lifetime "tails" in their decay curves.[22] Any higher series member that might cascade is well above the first ionization limit and will presumably autoionize. Also, production of higher members such as $2s2p^3 3p$ would require the simultaneous excitation of one electron and ionization of another and the cross section would be lower than for ionization alone.

The lifetime results corroborate the multielectron theory calculations of Westhaus and Sinanoğlu.[18] Such a theoretical method or an equivalent is necessary to treat the large amount of electron correlation in the "$2s2p^4$" configuration. A beam-foil lifetime determination of 834 Å by Bickel[33] is in disagreement with the 834-Å lifetime measured here. Probably the lifetime given by Bickel applies more nearly to the O IV transitionat the same wavelength.

1304-Å O I

The rest of this paper is about this multiplet. It consists of three lines with upper state $2p^3 3s\ ^3S^0$ with wavelengths 1302.1686-, 1304.8575-, and 1306.0286-Å[34] going down to the ground term ^3P with $J = 2$, 1, and 0, respectively. It is known on theoretical[31] and experimental[35] grounds that the intensities of the three lines are in the ratio 5:3:1. The lifetime of 1.82 ± 0.05 nsec given in Table I has been previously reported[36] and is an average of about 50 determinations made with various experimental parameters. Each lifetime determination is the slope of the "steep" exponential component as indicated in Fig. 1. The standard deviation estimate given by FRANTIC for each determination was generally less than 0.07 nsec. Decay curves were recorded on various occasions using CO, NO, O_2, and H_2O as sample gases, with both the diode and triode excitation source, with electron energies between threshold and 300 eV, with cathode emission currents between 0.5 and 10 mA, with gas pressures between 0.1 and 30 μ, and with pulse widths from 2 to 20 nsec. No significant variation in the lifetime was discovered as a function of the above parameters. Figure 3 illustrates the extent of pressure effects in H_2O.

Other determinations of the 1304-Å transition probability were listed in Ref. 36. We shall discuss here the f-value measurement of Parkes,

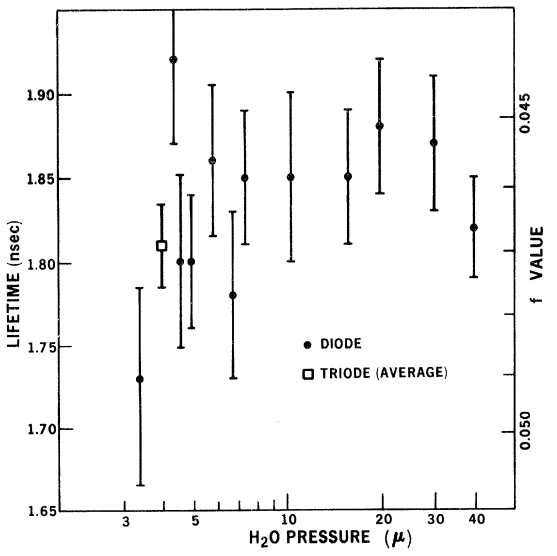

FIG. 3. Lifetimes of O I 1304 Å measured in H_2O at various pressures. Error bars are ± standard deviation given by FRANTIC.

Keyser, and Kaufman[37] (PKK) because of its importance to atmospheric physics. PKK used an argon discharge with a small amount of O_2 added as a source of 1304-Å radiation. Atomic oxygen concentration in an absorption cell was determined by gas titration techniques ($N + NO \rightarrow N_2 + O$). By assuming Doppler profiles of the emission lines and absorption probabilities, an f value of 0.021 ± 0.003 was determined which compares poorly with $f = 0.0463 \pm 0.0012$ given by a lifetime of 1.82 nsec. However, recent work by Parkes, Lin, and Kaufman[38] with a different light source (He + a little O_2) yields an f value of "about 0.045." The explanation seems to be that collisions with argon metastables were producing fast oxygen atoms in the $^3S^0$ excited state, thereby negating the Doppler-Doppler assumption. Thus, the lesson is that discharge light sources may emit lines with non-Doppler profiles because of energy transfer collisions.

We should also mention the recent measurements of the product of f value and Stark width for this multiplet by Morris and Garrison.[39]

Two-Level Cascade Analysis

The use of only two exponentials in fitting decay curves is obviously an approximation. Methods that have been used to handle the cascading problem in electron excitation include working at threshold,[40] detecting the delayed coincidence between the outgoing photon and (a) cascading photons[41] or (b) specific energy loss in the exciting electron.[42]

Bennett and Kindlmann[40] point out that for transitions to the ground configuration, the problem is less serious than for transitions between excited states. We find that in the case of 1304 Å, this is because of the wide separation between the $O(3p)$ and $O(3s)$ lifetimes and the observed fact that in the dissociative excitation of oxygen containing molecules, the $n = 3$ atomic levels receive most of the excitation.

The long cascade tails on the 1304-Å decay curves were found to be unusually straight and to have large amplitudes compared, say, with the tails of the rare-gas decay curves.[16,21] The average lifetime of this second exponential is 35.0 ± 1.0 nsec. This is in excellent agreement with the NBS value[12,43] of 35.7 ± 3.6 nsec for the $3p^3P$ term which radiates the multiplet 8446.5 Å (8447 Å). Least-square fits with three components did not establish a significant third exponential. Let us assume that the only cascade into the 1304-Å upper state (3s) is by the 8447-Å transition (3p). This assumption is based on (i) the statistically viable fit obtained with a two-cascade model and the absence of a third component; (ii) the observed independence of lifetimes from variations in the various experimental and analytical parameters; and (iii) the direct measurement of secondary cascades (Sec. V) gives ~2% contributions. The task now is to determine the relative rates of 3p and 3s excitation from an analysis of the observed decay curves. In Fig. 1, the set of points marked "cascade contribution" were calculated from the formalism to be outlined. This cascade contribution forms a curve which divides the fast response from the slow (cascade) response. Qualitatively, the cascade ratio $\sigma(3p)/\sigma(3s) \equiv \beta$ is given by the area under the curve divided by the area above the curve; corrected for decay rates, pulse width, etc.

We shall now show that the cascade ratio β can be found in terms of a zero of the Laplace transform of the observed decay curve, $F(t)$. The states 3p and 3s are represented in Fig. 4 as transfer functions $(1+ST)^{-1}$ and $(1+S\tau)^{-1}$, respectively, where S is the usual Laplace-transform (LT) variable. We neglect "other" cascades δ and ϵ. If the exciting pulse is $f(t)$ with a LT, $f(s)$, we can write by inspection of Fig. 4 the expected LT of $F(t)$ as

$$F(S) = f(S)\,(1+S\tau)^{-1}\,[1+\beta/(1+ST)]. \qquad (1)$$

We note that $F(S)$ has a zero at $-ST = 1+\beta$. Since $F(t)$ is the observed function, if we can compute its LT for real S and find a zero at negative S, our problem of finding β is solved. However, substitution of $F(t)$ into the integral definition of $F(s)$ does not work because the integral does not converge near $-ST = 1+\beta$. We can bypass the convergence problem by replacing the numerical $F(t)$ with the analytical form of its least-square approximation

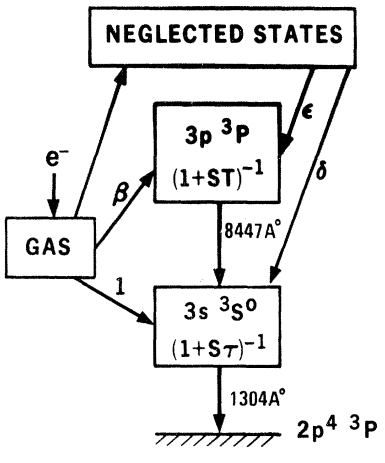

FIG. 4. Schematic of cascade analysis for O I 1304 Å. Electrons onto an oxygen-containing gas produce relative excitation rates 1, β, δ, and ϵ as shown. The variable S is the Laplace-transform variable.

for $t > t_0$. Hence, the integral defining $F(S)$,

$$F(S) = \int_0^\infty F(t) e^{-St}\, dt, \tag{2}$$

is replaced by

$$F(S) = \int_0^{t_0} F(t) e^{-St} dt + e^{-St_0}\left(\frac{\tau a_\tau}{1+S\tau} + \frac{T a_T}{1+ST}\right), \tag{3}$$

where t_0 is the time at which the fit begins. The least-square fit gives a function

$$F(t) = a_\tau e^{-(t-t_0)/\tau} + a_T e^{-(t-t_0)/T}, \quad \text{for } t > t_0.$$

The term after the first plus sign in (3) can be considered as an analytic continuation into the region where (2) diverges. For numerical reasons, the "depoled" function

$$F_1(S) \equiv F(S)\ (1+S\tau)(1+ST)\, e^{St_0}$$

was searched for the position of *its* zero. It is found, using experimental decay curves, that the zero crossing at $-ST = 1+\beta$ is essentially independent of excitation pulse width.

A generalization of this technique to arbitrary, N-level cascade systems is given in Sec. VII.

Measured values of cascade ratio β are given in Fig. 5 for various voltages and four gases.

IV. METHOD: ABSOLUTE CROSS SECTIONS

The absolute cross sections were measured using fairly conventional dc techniques. Review articles[44,45] and Kieffer's[46] recent compilation of excitation functions stress the importance of reducing systematic errors.

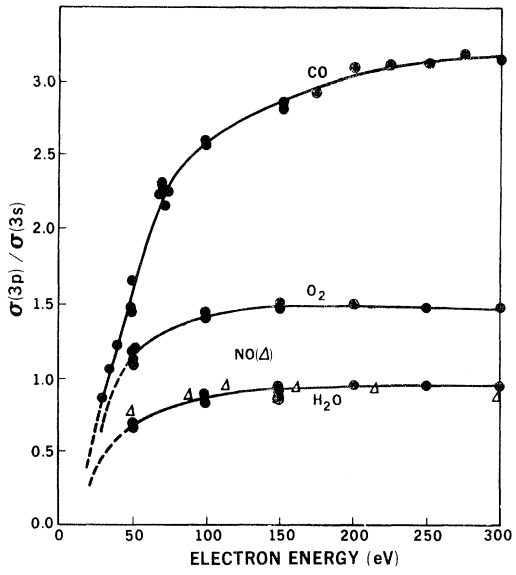

FIG. 5. O I 1304 Å, cascade ratio versus electron energy for $e^- + H_2O$, NO, O_2, and CO. Smooth curves are drawn for H_2O, O_2, and CO.

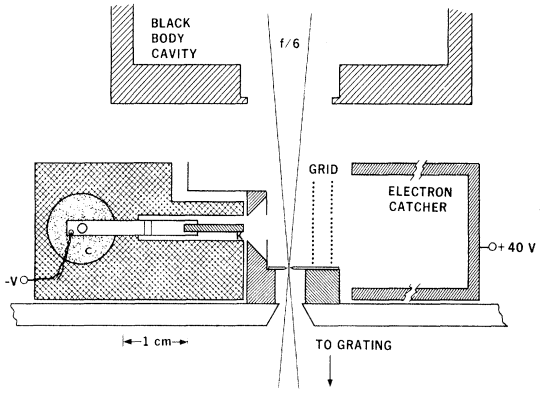

FIG. 6. Cross section of electron source used for cross-section measurements. K, tungsten ribbon cathode. C, ceramic insulator. Grid, 95% transparent. V is the nominal electron energy.

Hardware

The electron "beam" excitation source (Fig. 6) is backed up by a copper blackbody cavity used as a radiation standard. For the measurements at 3914 and 4368 Å, an Eppley-calibrated tungsten strip lamp was used as a radiance standard. The temperature of the copper blackbody was measured with three reference-grade platinum thermocouples. The cavity was blackened with an alcohol suspension of acetylene black, sprayed on with an air brush.[47] (Flame-applied soot is a very poor heat conductor.) The cavity was heated with resistance wire insulated with boron nitride.

The entrance slit (~ 300 μ wide) of an 0.3-m monochromator was imaged onto the beam, perpendicular to it. The physical slit indicated in Fig. 6 is ~ 1 mm wide and serves only as stray light baffle. An additional slit with width $\Delta l' \sim 0.32$ cm was placed perpendicular to the entrance slit, movable along the length of the entrance slit, and was used to scan the beam brightness profile, to check the uniformity of the detector sensitivity, and to define the slit length Δl [see Table II and Eq. (5)] when the blackbody intensity was measured. The photomultiplier at the exit slit was either a CO_2 cooled ITT FW-118 or an Amperex 56DUVP. Photoelectron pulses were recorded with a rate meter, with a frequency counter, or accumulated in the memory of a multichannel scaler as a function of log electron voltage. A Wratten 25-A filter was used as an order separator for 8447 Å.

The source was immersed in sample gas in a blind arm of a slow-flowing feed system. Pressure was measured with an MKS "Barytron" capacitance manometer, equipped with an electrostatic refer-

TABLE II. Cross-section parameters and error estimates.

Variable	Definition	Assumed values	Estimated limits of systematic error[a]
λ	Wavelength	8446.76 Å	···
T_B	Blackbody temperature	731 °K–873 °K	2 °K
ϵ	Blackbody emissivity	0.98	2%
$F(\lambda, T_B)$	Planck function; Eq. (4)	$8–400\times10^8$ cm^{-2} A^{-1} sec^{-1}	4%
R_B	Photoelectron rate, blackbody	$\sim 10^2–10^5$ sec^{-1}	1%
Δl	Length of optical slit	0.318 cm	2%
T_S	Source gas temperature	~310 °K	1%
T_G	Pressure gauge temperature	298 °K	···
$(T_G/T_S)^{1/2}$	Thermal transpiration factor	0.984	1%
$P\mu$	Gas pressure in μ Hg	0.1–10.0	3%
e	Electron charge	1.60×10^{19} C	···
I	dc electron trap current	50–1000 μA	10%
$R_S\Delta\lambda$	Area under scanned spectral line	$10^2–10^4$ Å sec^{-1}	1%
	Effect of secondary processes		5%
β	Cascade ratio	0.4–3.0	
$(1+\beta)/\beta$	uv normalization factor	3.5–1.3	5%
	Possible error[b]		41%
	Root-square error[b]		14%

[a]By δ error, one means a factor of $(1+\delta)^{\pm1}$.
[b]The corresponding values less the 5% uv normalization error are 36 and 13%, respectively.

ence calibration.

Most of the surfaces in the source were blackened with flame-applied soot in order to suppress stray light and reflected electrons.[48]

Cross-Section Formula

Table II lists the experimental variables which were used to determine the absolute excitation cross sections at 83 eV. After measurements of spectral line area, gas pressure, and electron current, the blackbody was warmed up to a convenient temperature and, with the Δl slit inserted, the observed count rate recorded. The radiance standard was the Planck function

$$F(\lambda, T) = 2c\lambda^{-4}(e^{a/\lambda T}-1)^{-1}, \qquad (4)$$

where $a = 1.4388$ cm °K, c is the velocity of light, and $F(\lambda, T)$ is expressed in photon rate per area per solid angle per wavelength interval. When the tungsten strip lamp was used, the calibration furnished by the Eppley Co. was converted to these units. Assuming isotropic radiation from the electron beam, the cross section σ is given for our geometry in terms of the variables of Table II by

$$\sigma = 4\pi e\left[\left(\frac{T_G}{T_S}\right)^{1/2}\frac{T_S}{9.65\times10^{15}\,^\circ\mathrm{K\,cm^3}}\right]\times\left[\frac{R_S\Delta\lambda}{P_\mu I}\right]\left[\frac{F(\lambda, T_B)\Delta l}{R_B}\right]. \qquad (5)$$

The first bracketed term converts the pressure gauge reading (P_μ) to particle density. The second bracketed term is a relative cross section which is found to be reasonably independent of pressure and electron current. The third bracketed term is a measure of the monochromator-detector efficiency and is found to be constant from day to day if the geometry is not changed. It is also found to be independent of T_B. The width Δl of the movable stop is the vertical height of the *image* of the physical stop at the electron beam position. The stop is in place only during measurements of R_B. In order for (5) to be valid, the monochromator detector has to have constant sensitivity across the beam profile. This was assured by proper geometrical adjustment and verified by scans of the blackbody radiation across the slit length.

If we measure the 8447-Å cross section according to (5), the 1304-Å cross section can be obtained by multiplying $\sigma(8447)$ by $(1+\beta+\delta+\epsilon)/(\beta+\epsilon)$, where the Greek letters are the relative cross sections defined in Fig. 4. We have chosen to neglect δ and ϵ and thus the conversion factor that is used is $(1+\beta)/\beta$. From considerations discussed in Sec. V, $\delta \sim 2\%$. The "secondary cascades" with strength ϵ come from states that make strong transitions to the ground state. From the observed strength of these transitions and from calculated branching ratios,[12] it is estimated that $\epsilon < 10\%$.

An analysis of the error caused by neglecting ϵ and δ is complicated because the β obtained from the computer analysis will be affected in a complicated way by the presence of these additional cascades. A numerical study was made using calculat-

ed decay curves with a third exponential component representing secondary cascades with lifetime T_1 and strength ϵ. The conclusion was that such errors are introduced only to second order in ϵ and in $(T_1 - T)/T$. For reasonable values of T_1 and ϵ, the error in σ(1304 Å) would be ~ 2% due to the presence of an ϵ-type cascade.

Polarization Is Not Observed

The 1304-Å radiation will not be polarized because it comes from an $L = 0$ term ($^3S^0$). The 8447-Å radiation could in principle exhibit polarization and so the polarization was measured. Again, the fine structure[49] was not resolved. A Polaroid "HR polarizing technical filter" was placed in the optical beam between the source and the monochromator and intensity measurements were made at 45° intervals in filter rotation. A harmonic analysis of the data yielded an (instrumental) polarization of 19.5% for measurements on the blackbody radiation. The 8447-Å radiation detected from CO showed 19.5 ± 0.5% polarization at six electron voltages between 60 and 300 V. The conclusion is that the 8447-Å radiation from CO is polarized less than ½%. This negative result was obtained at pressures of 3.6 and 0.32 μ.

Since Van Brunt and Zare[50] argue that atomic radiation would in general exhibit polarization in a simple dissociative excitation process, one might take the absence of polarization as a plausibility argument for the presence of several dissociating levels. This is plausible anyway. No further polarization measurements were made with O_2, NO, or H_2O.

As a practical matter, the absence of polarization simplifies the cross-section determination because the radiation will be isotropic.

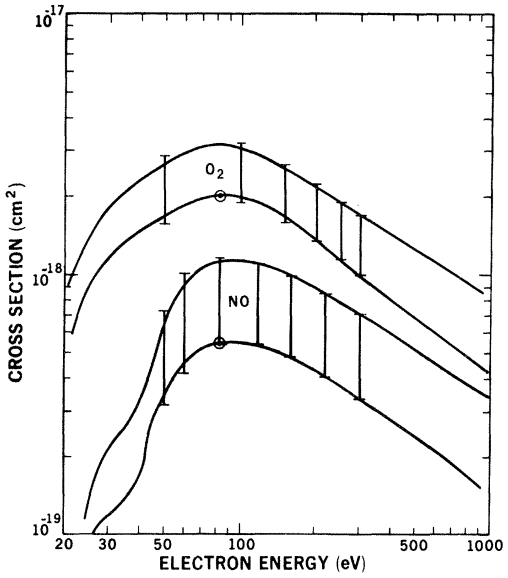

FIG. 7. Absolute cross section for electron impact on O_2 and NO. The solid curves are relative measurements positioned by the absolute measurement at 83 eV. In each set, the upper curve is for 1304 Å, the lower for 8447 Å. The vertical bars determine the spacing of the two curves. These bars are determined from the cascade analysis and have length $(1+\beta)/\beta$.

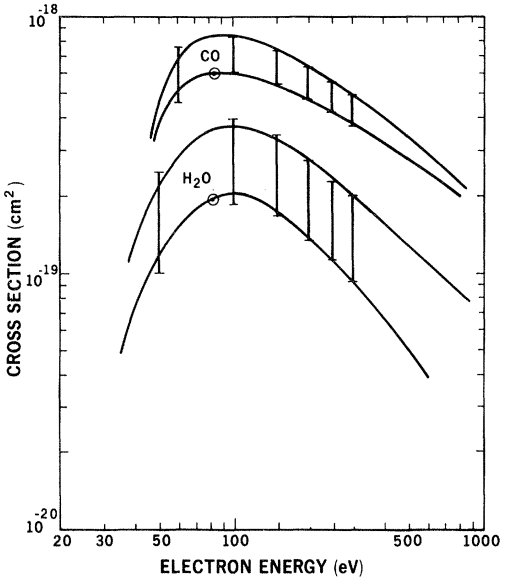

FIG. 8. Absolute cross section for electron impact on CO and H_2O. See caption of Fig. 7 for explanation.

V. RESULTS: CROSS SECTIONS

Figures 7 and 8 are log-log plots of the measured excitation functions for 8447 and 1304 Å. The unbroken curves are drawn through 256 points, logarithmically spaced in voltage. Statistical noise in the original points was ~ 5%. The voltage scale may be in error by two volts because of space charge and contact potentials.

The uv normalization factor $(1+\beta)/\beta$ establishes the length of the bars which were used to establish the vertical separation of the 8447- and 1304-Å curves. It can be seen that with respect to the high-energy values, the $(1+\beta)/\beta$ values are too large (β too small) at low energies. It is believed that this is caused by poor energy definition in the pulsed electron source. Thus, the curves of Fig. 5 should rise more steeply from threshold and saturate more sharply.

Table III gives the absolute cross sections at 83 and 100 eV. The measurements at 4368 and 3914 Å were made to provide extra information.

TABLE III. Absolute electron excitation cross sections.

Sample gas	λ (Å)	σ(83 eV) (10^{-18} cm^2)	σ(100 eV) (10^{-18} cm^2)
CO	8447	0.60	0.59
O_2	8447	2.02	2.00
NO	8447	0.55	0.55
H_2O	8447	0.19	0.20
CO	1304	0.85	0.84
O_2	1304	3.18	3.05
NO	1304	1.14	1.14
H_2O	1304	0.37	0.37
CO	4368	0.012	···
O_2	4368	0.047	···
N_2	3914	17.5	15[a]

[a]Other authors at 83 V, Ref. 43, p. 145, upper set.

3914-Å N_2^+

This measurement was included as a check of cross-section method. The tungsten strip lamp was used with a calibrated neutral density filter as a radiance standard and this introduces another ~10% uncertainty in the cross section. The band profile was integrated from a spectral scan between 3890 and 3920 Å. Previous measurements of the cross section, compiled by Kieffer,[46] fall into two groups which are a factor of about 2.7 apart. The value measured here and listed in Table III is 17% higher than the mean of the upper group.

4368-Å O I

This transition is the $4p$-$3s$ transition of the cascade type labeled δ in Fig. 4. An examination of Table III shows that in CO and O_2, its cross section at 83 eV is about 2% of the 8447-Å cross section. The $5p$-$3s$ cascade at 3692 Å was not observable above the detector background. Thus we may take $\delta \sim 0.02$ for the purpose of estimating the error in the two-state cascade assumption.

Quintet Levels Observed

The multiplet 7774 Å $3p\,^5P \rightarrow 3s\,^5S^0$ is also observed with the same order of magnitude of cross section as the 8447-Å triplet multiplet. Thus, it would be expected that the long-lived $3s\,^5S^0$ term is excited by ~100-eV electrons in roughly the same amount as the $3s\,^3S^0$.

Bethe-Born: O_2

Vroom and DeHeer[2] use the Bethe-Born approximation to relate photoabsorption cross sections to the high-energy behavior of electron excitation functions. In their notation, the electron excitation function is expected to behave as $\sigma \propto M_n^2(\ln cE)/E$, where E is the electron energy, c is a constant, and M_n^2 is an integral over the photodissociation cross section. By determining the slope of a straight line in a so-called "Bethe plot," we obtain, from the O_2 data of Fig. 7, $M^2(1304\text{ Å}) = 0.043$ and $M^2(8447\text{ Å}) = 0.021$.

In order to get an M^2 value from photoabsorption measurements, we have to isolate that portion of the total photoabsorption cross section which leads to dissociation yielding 1304-Å radiation. A study of Beyer and Welge's[8] fluorescence spectra indicates that most of the 1304-Å radiation results from absorption of photons with energies between 16.0 and 18.0 eV. This conclusion implies that the dissociating excited atoms will have kinetic energies in the neighborhood of 1 eV. Integrating the photodissociation cross section of Matsunaga and Watanabe[7] between 16 and 18 eV yields M^2 (photo) = 0.062. The difference between this value and $M^2(1304\text{ Å}) = 0.043$ determined from the cross section of Fig. 7 can be explained by any or all of the following: (a) Errors exist in the measurements. (b) The Bethe-Born formalism is not exact. (c) The photodissociation cross section between 16 and 18 eV includes processes which lead to quintet-state oxygen atoms.

This dissociative process is an important component of the total absorption spectrum of O_2.

VI. ERRORS IN CROSS SECTION

As summarized in Table II, the accuracy in the absolute cross sections is in the order of 15% with errors of 40% "possible" but not probable. The "estimated limits of systematic error" given in the last column of Table II are educated guesses based on measurements of variations with system parameters, on model calculations (e.g., quenching rates), and on manufacturer's specifications. The dominant errors are the uncertainty in the electron beam current collection efficiency, the effect of secondary processes, and the accuracy of the cascade ratio β used to make the infrared-to-uv normalization. The cross sections for H_2O are probably uncertain by another 5% or so because of pressure measurement errors caused by adsorption in the gauge and gauge lines.

In varying the electron catcher bias from −10 to 100 V, the collected electron current varied approximately 10%. The bias was set at 40 V for the measurements. Given the 10% variation, it is unclear how much of the change is due to extraneous effects such as collection of secondary electrons rather than saturation of collection efficiency.

Variations in apparent cross section were observed as a function of pressure and never exceeded 10%. The values reported are based on extrapolations to zero pressure. A quenching cross section of 10^{-16} cm^2 is approximately correct for explaining the observed variation if the dissocia-

ting oxygen atom has an energy of 1 eV.

Relative cross sections for 1304 Å were measured at 85 eV in H_2O, CO, NO, and O_2 by measuring R_S/P_μ at fixed electron current and fixed monochromator setting. These relative values, normalized to have the same geometric mean as the values from Table III, agree with the cascade analysis values within 10%.

APPENDIX: *N*-STATE CASCADES

We are given the observed decay curve $F(t)$ and the branching ratios B_{kj} from states k to states j. We take the model that a finite number (N) of states decay exponentially with reciprocal lifetimes $1/\tau_k = \alpha_k$ (all distinct). Let us call the excitation pulse $f(t)$, assuming the direct excitation rate of state i to be $\beta_i f(t)$. The problem then is to find the β_i. We begin by picking some value of time t_0, large enough to ensure that the excitation $f(t_0) = 0$ and then we use FRANTIC to characterize the tail of the decay curve as a sum of exponentials. That is,

$$F(t)\big|_{t>t_0} = \sum_i a_i e^{-\alpha_i (t-t_0)} ,$$

where the a_i might be called the amplitudes at $t = t_0$. We need, however, a more basic set of amplitudes, the amplitudes b_i obtained in response to a δ function. Denoting the Laplace transform of $F(t)$ by $F(S)$, we can write

$$F(S) \equiv \int_0^{t_0} e^{-St} F(t)\,dt + e^{-St_0} \sum_i \frac{a_i}{\alpha_i + S}$$
$$= f(S) \sum_i \frac{b_i}{\alpha_i + S} . \qquad (6)$$

We want to find a set of b_i (on a relative scale) such that the right-hand equality in (6) holds where $F(S) = 0$. The computer was programmed to search for $N-1$ real numbers S_l which give zeros of the center expression. Arbitrarily setting $b_1 = 1.0$, we then obtain an $N-1$-by-$N-1$-dimensioned set of linear equations by rewriting the right-hand expression of (6):

$$\sum_{i=2}^{N} \frac{b_i}{\alpha_i + S_l} = \frac{1}{\alpha_1 + S_l} , \qquad l = 1, 2, \ldots, N-1. \qquad (7)$$

We solve for the b_i. Thus, in spite of the unknown excitation pulse shape, we obtain the response to a δ function.

The final step is to calculate the relative excitation rates β_i of the various states by developing the (linear) relation between the β_i and the b_i, and then inverting. The coefficients obtained in cascades of exponentially decaying states are well known, [51] but complicated. An algorithm dealing with pairs of interacting states was used to set up a machine computation. We use a conventional partial fraction expansion. Given a cascading "signal" which is decaying exponentially with lifetime τ_k, the population of state j due only to this cascade into it is proportional to

$$(\alpha_k + S)^{-1} (\alpha_j + S)^{-1} \equiv X_{kj}/(\alpha_k + S) - X_{kj}/(\alpha_j + S) ,$$

where $X_{kj} = (\alpha_k - \alpha_j)^{-1}$.

Thus, we have described the interaction of lifetimes k and j in a cascade situation. The response of state j to direct excitation is $\beta_j/(\alpha_j + S)$. We are going to compute a set of numbers P_{il}^k so that the i lifetime component of state k's radiation is

$$\frac{b_i^k}{\alpha_i + S} = \frac{1}{\alpha_i + S} \sum_l P_{il}^k \beta_l , \qquad (8)$$

where the b_i^k are the b_i [Eq. (6)] that would be obtained by locating the zeros of an $F(S)$ measured from a state k. With the indices arranged so that higher-energy states have the higher indices we get the following development of P_{jl}^k by following all cascade channels and pair interactions:

$P_{jj}^j = 1$, direct excitation

$i > j$: $P_{il}^j = \sum_{k>j} P_{il}^k B_{kj} \alpha_k X_{ij}$,

transmission of lifetime k

$l > j$: $P_{jl}^j = -\sum_{k \geq i} \sum_{k>j} P_{il}^k B_{kj} \alpha_k X_{ij}$,

creation of negative component by another component passing through.

The complete set P_{il}^k can be computed by applying the above equations starting with the highest states. Then the linear equation set (9) is solved for the β_i.

FORTRAN coding of the above process was straightforward except for a numerical approximation used to obtain the integral in (6). Since only the average values A_k of $F(t)$ are known over the time intervals $[T_k, T_k + \Delta T_k]$, the integral

$$I_K \equiv \int_{T_K}^{T_K + \Delta T_K} e^{-St} F(t)\,dt \qquad (9)$$

is approximated by

$$I_K \sim e^{-S(T_k + \Delta T_k/2)} [A_K - (A_{k+1} - A_{k-1}) S \Delta T_k/24],$$

which is correct to first order in $S\Delta T_k$. Typically, $S_l \Delta T_K \sim 0.1$.

The complete FORTRAN program has been added to FRANTIC and has been tested on independently computed decay curves and has been checked for consistency on observed decay curves. It has not been tested on cases where negative exponential amplitudes are in the decay curves (negative b_i).

Further analysis should be done in order to calculate statistical error estimates for the β_i.

[1]Wavelengths and multiplet numbers are from R. L. Kelly, NRL Report No. 6648 (U.S. GPO, Washington, D.C., 1968).

[2]D. A. Vroom and F. J. de Heer, J. Chem. Phys. 50, 580 (1969).

[3]G. H. Dunn, R. Geballe, and D. Pretzer, Phys. Rev. 128, 2200 (1962).

[4]J. W. McGowan, J. F. Williams, and D. A. Vroom, Chem. Phys. Letters 3, 614 (1969).

[5]E. A. Lassettre, A. Skerbele, M. A. Dillon, and K. J. Ross, J. Chem. Phys. 48, 5066 (1968).

[6]J. Geiger and B. Schröder, J. Chem. Phys. 49, 740 (1968).

[7]F. M. Matsunaga and K. Watanabe, Sci. Light 16, 31 (1967).

[8]K. D. Beyer and K. H. Welge, J. Chem. Phys. 51, 5323 (1969).

[9]W. Sroka, Z. Naturforsch. 23a, 2004 (1968).

[10]K. Ziock, in *Methods of Experimental Physics* (Academic, New York, 1967), Vol. 4, Part B, p. 214ff.

[11]B. M. Miles and W. L. Wiese, NBS Special Publication No. 320 (U.S. GPO, Washington, D.C., 1970).

[12]W. L. Wiese, M. W. Smith, and B. M. Glennon, Report No. NSRDS-NBS-4 (U.S. GPO, Washington, D.C., 1966).

[13]W. L. Wiese, M. W. Smith, and B. M. Miles, Report No. NSRDS-NBS-22 (U.S. GPO, Washington, D.C., 1969).

[14]D. W. O. Heddle and R. G. W. Keesing, in *Advances in Atomic and Molecular Physics*, edited by D. R. Bates (Academic, New York, 1968), Vol. IV, p. 267ff.

[15]G. M. Lawrence, Research Communication No. 93, Douglas Advanced Research Laboratories, 1969 (unpublished).

[16]G. M. Lawrence, Phys. Rev. 175, 40 (1968).

[17]P. C. Rogers, MIT Laboratory for Nuclear Science, Technical Report No. 76 (NYO-2303), 1962 (unpublished).

[18]P. Westhaus and O. Sinanoğlu, Phys. Rev. 183, 56 (1969).

[19]M. A. Duguay and J. W. Hansen, Opt. Commun. 1, 254 (1969).

[20]G. M. Lawrence and B. D. Savage, Phys. Rev. 141, 67 (1966).

[21]G. M. Lawrence and H. S. Liszt, Phys. Rev. 178, 122 (1969).

[22]G. M. Lawrence, Phys. Rev. 179, 134, (1969).

[23]B. D. Savage and G. M. Lawrence, Astrophys. J. 146, 940 (1966).

[24]J. E. Hesser, J. Chem. Phys. 48, 2518 (1968).

[25]G. Herzberg, *Atomic Structure and Atomic Spectra* (Dover, New York, 1944), p. 163.

[26]R. E. Huffman, J. C. Larrabee, and Y. Tanaka, J. Chem. Phys. 46, 2213 (1967).

[27]M. E. Rudd and K. Smith, Phys. Rev. 169, 79 (1968).

[28]F. J. Comes, F. Speier, and A. Elzer, Z. Naturforsch. 23a, 125 (1968).

[29]P. Feldman and R. Novick, Phys. Rev. 160, 143 (1967).

[30]S. Obi and S. Yanagawa, Publ. Astron. Soc. Japan 7, 125 (1955).

[31]R. H. Garstang, Proc. Cambridge, Phil. Soc. 57, 115 (1961).

[32]A. W. Weiss, Phys. Rev. 162, 71 (1967).

[33]W. S. Bickel, Phys. Rev. 162, 7 (1967).

[34]G. Herzberg, Trans. Int. Astron. Union 11A, 97 (1962).

[35]W. R. Ott, Bull. Am. Phys. Soc. 15, 45 (1970).

[36]G. M. Lawrence, Can. J. Chem. 47, 1856 (1969).

[37]D. A. Parkes, L. F. Keyser, and F. Kaufman, Astrophys. J. 149, 217 (1967).

[38]D. A. Parkes, C. C. Lin, and F. Kaufman (private communication).

[39]J. C. Morris and R. L. Garrison, Phys. Rev. 188, 112 (1969).

[40]W. R. Bennett, Jr., and P. J. Kindlmann, Phys. Rev. 149, 38 (1966).

[41]R. D. Kaul, J. Opt. Soc. Am. 56, 1262 (1966).

[42]R. E. Imhof and F. H. Read, Chem. Phys. Letters 3, 652 (1969).

[43]J. E. Solarski and W. L. Wiese, Phys. Rev. 135, A1236 (1964).

[44]B. L. Moiseiwitsch and S. J. Smith, Rev. Mod. Phys. 40, 238 (1968).

[45]L. J. Keiffer and G. H. Dunn, Rev. Mod. Phys. 38, 1 (1966).

[46]L. J. Kieffer, Atom. Data 1, 120 (1969).

[47]Various methods of calculating cavity emissivity are outlined in *Handbook of Military Infrared Technology*, edited by W. L. Wolfe (Superintendent of Documents, U. S. GPO, Washington, D. C., 1965), Chap. 3.

[48]Paul Marmet and L. Kerwin, Can. J. Phys. 38, 787 (1960).

[49]L. W. Parker and J. R. Holmes, Phys. Rev. 90, 142 (1953).

[50]R. J. Van Brunt and R. N. Zare, J. Chem. Phys. 48, 4304 (1968).

[51]L. J. Curtis, Am. J. Phys. 36, 1123 (1968).